
1 The relative importance of antecedent soil moisture and precipitation
2 in flood generation in the middle and lower Yangtze River basin

3

4 Qihua Ran¹, Jin Wang², Xiuxiu Chen², Lin Liu², Jiyu Li², Sheng Ye^{2*}

5

6 ¹ State Key Laboratory of Hydrology-Water Resources and Hydraulic Engineering,
7 Hohai University, Nanjing 210098, China

8 ² Institute of Water Science and Engineering, College of Civil Engineering and
9 Architecture, Zhejiang University, Hangzhou 310058, China

10

11 * Corresponding author: Sheng Ye

12

13 Email address of the corresponding author: yesheng@zju.edu.cn

14

15 September 8, 2022

16

17

18

19 **Abstract**

20 Floods have caused severe environmental and social economic losses worldwide in
21 human history, and are projected to exacerbate due to climate change. Many floods are
22 caused by heavy rainfall with highly saturated soil, however, the relative importance of
23 rainfall and antecedent soil moisture and how it changes from place to place has not
24 been fully understood. Here we examined annual floods from more than 200
25 hydrological stations in the middle and lower Yangtze River basin. Our results indicate
26 that the dominant factor of flood generation shifts from rainfall to antecedent soil
27 moisture with the increase of watershed area. The ratio of the relative importance of
28 antecedent soil moisture and daily rainfall (SPR) is positively correlated with
29 topographic wetness index and has a negative correlation with the magnitude of annual
30 floods. This linkage between watershed characteristics that are easy to measure and the
31 dominant flood generation mechanism provides a framework to quantitatively estimate
32 potential flood risk in ungauged watersheds in the middle and lower Yangtze River
33 basin.

34 **Key words:** flood generation, scaling effect, topographic wetness index

35

36

37 **1. Introduction**

38 Flooding is one of the most destructive and costly natural hazards in the world, resulting
39 in considerable fatalities and property losses (Suresh et al., 2013). River floods have
40 affected nearly 2.5 billion people between 1994 and 2013 worldwide (CRED, 2015),
41 and caused 104 billion dollars losses every year (Desai et al 2015). The damages may
42 be further exacerbated by increasing frequency and intensity of extreme rainfall events
43 according to climate change projections (IPCC 2012; Ohmura and Wild 2002). Flood
44 control infrastructures and more accurate predictions are needed to reduce flood
45 damages, which requires better understanding of the underlying mechanism of flood
46 generation as well as the drivers of change (Villarini & Wasko 2021).

47 Numerous studies have been conducted to investigate the cause of floods across
48 the world (Bloschl et al 2013; Munoz et al 2018; Zhang et al 2018). Many studies
49 focused on examining the environmental and social characteristics that lead to specific
50 catastrophic flood events (Bloschl et al 2013; Liu et al 2020; Zhang et al., 2018). Others
51 concentrated on single locations, usually catchment outlets, to explore the influential
52 factors of floods and the future trends (Brunner et al., 2016; Munoz et al 2018). Yet
53 given the amount of data and time required, it is not practical to apply these detailed
54 studies to hundreds of catchments to generate an overview of the flood generation
55 mechanism at large scale.

56 Recently, researchers started to investigate the dominant flood generation
57 mechanisms at regional scales (Berghuijs et al 2019b; Do et al 2020; Garg & Mishra
58 2019; Smith et al 2018; Trambly et al 2021; Ye et al 2017). Most of these studies are
59 conducted in North America and Europe with well-documented long-term records
60 (Berghuijs et al 2016; Bloschl et al 2019; Do et al 2020; Musselman et al 2018; Rottler

61 et al 2020). Some research was conducted in China recently (Yang et al 2019; Yang et
62 al 2020), though such kind of work is still limited, further investigations are needed
63 given the considerable spatial heterogeneity and complexity in flood generation.

64 As the largest river in China, Yangtze River basin has long suffered from floods. In
65 summer 2020, 378 tributaries of the Yangtze River had floods exceeding the alarm level,
66 causing billions of dollars damage (Xia et al., 2021). With the increasing public
67 awareness, more accurate prediction is needed, which relies on better understanding.
68 However, due to the limitation of observations, there are only a few regional studies of
69 the flood generation mechanism in China, with few in the Yangtze River basin (Zhang
70 et al 2018; Yang et al 2019; Yang et al 2020). The large number of dams and reservoirs
71 built along the river further complicated the situation (Feng et al., 2017; Qian et al 2011;
72 Yang et al 2019).

73 Because of the relatively warm temperature, snowmelt has little impact on flood
74 generation in the Yangtze River basin (Yang et al 2020). Floods in the Yangtze River
75 basin usually occur during summer with relatively wet soil and high rainfall (Wang et
76 al 2021). Heavy rainfall with high antecedent soil moisture has also been identified as
77 dominant driver of floods across world (Beighuijs et al 2019b; Garg et al 2019;
78 Trambly et al 2021; Wasko et al 2020). Recently, studies started to examines the
79 relative importance of rainfall and antecedent soil moisture in flood generation
80 (Brunner et al., 2021; Wasko et al., 2021; Bennett et al., 2018; Bertola et al., 2021).
81 Quantitative evaluation of the relative contribution of rainfall and antecedent soil
82 moisture and its change across watersheds is still limited and currently unavailable in
83 China (Liu et al., 2021; Wu et al., 2015).

84 Based on the watersheds in the middle and lower Yangtze River basin, this study

85 attempts to explore the following questions: 1) is there a way to quantitatively describe
86 the relative importance of antecedent soil moisture and rainfall on flood generation; and
87 2) how would this combination of flood-generation rainfall and soil moisture vary
88 across watersheds, and what are the influential factors. Based on the observations and
89 model estimation (Section 2), the spatial distribution patterns of antecedent soil
90 moisture and rainfall were obtained and analyzed to investigate their individual
91 contribution to flood generation and the influential factors (Section 3). This allows for
92 further examination of the relative importance of antecedent soil moisture and rainfall
93 on flood generation and its linkage to watershed characteristics as well as its
94 implications to flood prediction (Section 4), all the results are summarized in Section 5.

95 **2 Methods**

96 **2.1 Study area**

97 The Yangtze River is the largest river in China, with a total length of 6,300 kilometers
98 and annual discharge of 920km^3 at the outlet (Yang et al., 2018). It drains through an
99 area of $1.8 \times 10^6 \text{ km}^2$, lying between $90^\circ 33'$ and $122^\circ 25'$ E and $24^\circ 30'$ and $35^\circ 45'$ N, and
100 is home to over 400 million people, most of which live in the middle and lower Yangtze
101 River basin (YZRB) (Cai et al., 2020). The elevation of the YZRB declines from west
102 to east: from over 3000m in Qinghai-Tibet Plateau, to around 1000m in the central
103 mountain region, and the 100m in Eastern China Plain (Wang et al., 2013). The
104 vegetation types in the YZRB are forests, shrubs, grassland and agricultural land,
105 accounting for 11.85%, 12.65%, 32.26% and 42.88% respectively. Grassland and
106 shrubs are the dominant vegetation in the middle and upper YZRB, while the
107 downstream YZRB is dominated by forests and agricultural land (Miao et al., 2010).
108 There are more than 51,000 reservoirs of different sizes in the whole basin, including

109 280 large ones (Peng et al., 2020).

110 Most of the YZRB is semi-humid and humid, with a typical subtropical monsoon
111 climate. The mean annual temperature is approximately 13.0 °C, varying from -4 °C
112 to 18°C downstream. The mean annual precipitation of the whole basin is about 1200
113 mm, increasing from 300mm in the western headwaters to 2400 mm downstream. (Li
114 et al., 2021). Most of the precipitation comes between June and September, the premise
115 of persistent heavy rain in the Yangtze River basin is the frequent activity of weak cold
116 air in the north (Tao et al., 1980) and the intersection of mid-latitude air mass and
117 monsoon air mass (Kato et al., 1985). Studies have found that both annual precipitation
118 and the frequency of extreme precipitation events have increased in the middle and
119 lower reaches of the Yangtze River (Qian et al., 2020; Fu et al., 2013). As a result, floods
120 have occurred frequently in the middle and lower reaches of the Yangtze River, where
121 most of the population in the YZRB live (Liu et al., 2018).

122 **2.2 Data**

123 In this work, we focus on the middle and lower reaches of the Yangtze River for the
124 high population density and increasing flood risk. The 30-meter digital elevation model
125 (DEM) was downloaded from Geospatial Data Cloud (<http://www.gscloud.cn/>), from
126 which the drainage area corresponding to the hydrological station was extracted by
127 ArcGIS. Daily precipitation data and temperature data between 1970 and 2016 from
128 247 meteorological stations within and near the YZRB were downloaded from China
129 Meteorological Data Network (<https://data.cma.cn/>) (Figure 1). The temperature data
130 was used to estimate potential evaporation. The observed precipitation and estimated
131 potential evaporation were interpolated into the whole YZRB using the Thiessen
132 polygon method (Meena et al., 2013). The interpolated precipitation and potential

133 evaporation were then averaged for the drainage area corresponding to each
134 hydrological station.

135 The daily streamflow data was collected from 267 hydrological stations from
136 Annual Hydrological Report of the People's Republic of China. Among which, 224
137 stations with at least 20 years records from both the period from 1970 to 1990 and the
138 period from 2007 to 2016 were selected, the data from 1990 to 2007 were not found in
139 online repository (see Figure S1 for data availability). Information of 361 reservoirs in
140 the middle and lower YZRB, including capacity and controlling area was downloaded
141 and extracted from the Global Reservoir and Dam database (GRanD) (Lehner et al
142 2011). Previous study showed that this database provides reliable information of middle
143 and large reservoirs in China (Yang et al 2021). Watersheds with more than 80% of the
144 drainage area under control reservoirs according to GRanD database and/or located
145 right downstream of reservoirs and water gates were considered as watersheds under
146 strong regulation (regulated watersheds).

147 **2.3 Calculation of hydrological and topographic characteristics**

148 *Potential evaporation estimation*

149 The temperature data was used to estimate potential evaporation following the
150 Hargreaves method (Allen et al., 1998; Vicente et al., 2014; Berti et al., 2014).

$$151 \quad ET_0 = 0.0023 \times (T_{max} - T_{min})^{0.5} \times (T_{mean} + 17.8) \times Ra \quad (1)$$

152 where ET_0 is potential evaporation (mm/d), T_{max} is the highest temperature ($^{\circ}\text{C}$), T_{min}
153 is the lowest temperature ($^{\circ}\text{C}$), T_{mean} is the mean temperature ($^{\circ}\text{C}$), and Ra is the outer
154 space radiation [$\text{MJ}/(\text{m}^2 \cdot \text{d})$], which can be calculated as follows:

155
$$Ra = 37.6 \times d_r \times (\omega_s \sin \varphi \sin \delta + \cos \varphi \cos \delta \sin \omega_s), \quad (2)$$

156 where d_r is the reciprocal of the relative distance between the sun and the earth, ω_s is
 157 the angle of sunshine hours, δ is the inclination of the sun (rad), φ is geographic
 158 latitude (rad). d_r , δ and ω_s can be calculated by the following formula:

159
$$d_r = 1 + 0.033 \times \cos\left(\frac{2\pi J}{365}\right), \quad (3)$$

160
$$\delta = 0.409 \times \sin\left(\frac{2\pi J}{365} - 1.39\right), \quad (4)$$

161
$$\omega_s = \arcsin(-\tan \varphi \tan \delta), \quad (5)$$

162 where J is the daily ordinal number (January 1st is 1).

163 *Soil water storage estimation*

164 The soil water storage was estimated based on the daily water balance (Berhuijs et al.,
 165 2016, 2019):

166
$$\frac{dS}{dt} = P - ET - \max(Q, 0), \quad (6)$$

167 Where S is the soil water storage (mm), which is initially set to 0. Due to the long term
 168 of simulation, the change of initial value would not significantly affect the results. P is
 169 precipitation (mm/d), Q is discharge normalized by area (mm/d), ET is evaporation
 170 (mm/d), which can be calculated from potential evapotranspiration (ET_0), where the
 171 soil water storage (S) is used as the upper limit of daily ET:

172
$$ET = \min(0.75 \times ET_0, S), \quad (7)$$

173 The estimation of soil water storage and ET are highly simplified and is not used for

174 prediction but to capture the first order of the temporal variation and the relative wetness
175 of soil in the study time period, which helps develop a framework that differentiates the
176 relative contribution of precipitation and soil moisture in flood generation.

177 *Topographic wetness index estimation*

178 Topographic wetness index was calculated to represent the combined impacts of
179 drainage area and topographic gradient (Alfonso et al., 2011; Grabs et al., 2009):

180
$$TWI = \ln(A_d/\tan\alpha), \quad (8)$$

181 where A_d is drainage area and α is topographic gradient estimated from DEM. TWI
182 represents the propensity of subsurface flow accumulation and frequency of saturated
183 conditions, thus can be used to predict relative surface wetness and hydrological
184 responses (Meles et al 2020). It is widely used to quantify topographic impact on
185 hydrological processes (i.e., spatial scale effects, hydrological flow path, etc.), as well
186 as in land surface models for hydrological, biogeochemical and ecological processes
187 (Sorensen et al 2006).

188 **2.4 Quantification of the relative importance of soil moisture and precipitation**
189 **during floods**

190 The maximum daily discharge of each year was selected as annual flood, which was
191 then averaged across years as the mean annual maximum flood (AMF). The observed
192 rainfall on that day and the estimated soil water storage at the day before AMF in each
193 year were also averaged across years as daily rainfall (P) and antecedent soil moisture
194 (S_0). Since almost all the AMFs in our study region come during rainy season when
195 rainfall comes in most of the days, it could be difficult to isolate the events of AMFs
196 among consecutive flow events. To avoid the bias that may be caused in event

197 separation, the soil moisture at the day before AMF was used as antecedent soil
198 moisture, instead of the day before the event of AMF. To examine the impacts from
199 long-lasting rainfall event, especially for the large watersheds with longer concentration
200 time, we also calculated the mean accumulated rainfall from two days (rainfall on the
201 flood day and the day before, P_2) to seven days before (weekly rainfall, P_7).

202 The percentile of antecedent soil moisture (S_0) was calculated to represent the
203 relative saturation of soil moisture in the time series; while the percentile of daily
204 rainfall (P) was estimated to show the relative intensity (P'), representing the relative
205 magnitude of rainfall events across time. The percentile of accumulated rainfall was
206 also calculated for the two-day to seven-day rainfall.

207 To quantify the relative importance of antecedent soil moisture and rainfall in flood
208 generation, the ratio between these two factors at the AMFs was derived: $SPR = S'/P'$.
209 When SPR is large, the antecedent soil moisture is much closer to the maximum, while
210 the daily rainfall is less extreme, floods are more affected by the antecedent soil
211 moisture. On the other hand, a smaller SPR indicates relatively larger magnitude of
212 rainfall comparing with antecedent soil moisture, that is, rainfall is more extreme and
213 influential in flood generation.

214 **3 Results**

215 **3.1 Spatial patterns of antecedent soil moisture and precipitation during floods**

216 Figure 2 shows the spatial distribution of the percentile of antecedent soil moisture and
217 daily rainfall during the annual maximum floods (AMFs) in the middle and lower
218 reaches of the Yangtze River. As we can see from Figure 2a, in the middle and lower
219 reaches of YZRB, when AMFs occurred, the percentile of antecedent soil saturation

220 was generally high, most of them are larger than 0.6: the farther away from the main
221 stream, the more saturated the soil was. On the other hand, along and near the main
222 stream and the delta, the antecedent soil saturation rate could be much smaller, even
223 less than 0.4.

224 Figure 2b shows the daily rainfall during the AMFs. As we can see, the percentile
225 of daily rainfall is relatively high (>0.8) at more than half of the study sites, while it is
226 small (<0.5) for the sites along the main stream and in the delta (Figure 2b). Comparison
227 between Figure 2a and b suggests that, except the sites on the main stream and in the
228 delta, sites with relatively high antecedent soil saturation rate (i.e., >0.8 , the blue dots)
229 during AMFs are also the ones with relatively small daily rainfall contribution (i.e.,
230 <0.8 , the light blue and cyan dots). That is, for these sites, the AMFs are usually
231 occurring at a much wetter condition while extreme rainfall at flood day is not necessary,
232 suggesting the relative importance of soil wetness. For the sites with both the percentile
233 of soil moisture and rainfall between 0.6 and 1, both the antecedent soil moisture and
234 rainfall play important roles in flood generation. As for the sites on the main stream and
235 in the delta, both antecedent soil moisture and rainfall are low during AMFs, this is
236 likely due to the regulations from large reservoirs and water gates.

237 **3.2 The scaling effect in the contribution of antecedent soil moisture and rainfall**

238 To further investigate the relative importance of antecedent soil moisture and rainfall in
239 flood generation and the potential influential factors, we examined their correlation with
240 catchment area (Figure 3). Given the complicated environmental and social impacts,
241 the regulated watersheds and sites on the main stream are presented separately (the
242 green dots and cyan dots in Figure 3 respectively). Our study will focus on the sites that
243 are not dominated by regulation (the blue dots in Figure 3), for simplicity, we will refer

244 them as natural watersheds.

245 As we can see from Figure 3, during the occurrence of AMFs, the percentile of
246 antecedent soil wetness increases with watershed area (p -value<0.001), while the
247 percentile of daily rainfall decreases with watershed area (p -value<0.001). That is, with
248 the increase of watershed size, antecedent soil moisture becomes more and more
249 saturated while the precipitation is less and less extreme during AMFs; suggesting the
250 rising contribution of antecedent soil moisture and declining importance of daily
251 precipitation in flood generation. As for the regulated watersheds (green dots in Figure
252 3), there is no clear correlation between drainage area and the percentile of antecedent
253 soil moisture or rainfall, which is understandable. Meanwhile, both the percentile of
254 antecedent soil moisture and rainfall decreases with watershed area for main stream
255 sites.

256 **3.3 The scaling impacts on accumulated rainfall**

257 The saturation of soil before floods could be due to previous rainfall events, and could
258 also be caused by accumulated rainfall in long-lasting rainfall events that eventually
259 generate floods (Xie et al., 2018). Figure 4 presents the correlation between the
260 percentile of accumulated rainfall and drainage area. When single day rainfall is
261 considered, it is negatively correlated with drainage area (Figure 3a); when accumulated
262 rainfall is considered, the correlation gradually shifts from negative to positive
263 correlation (Figure 4). For example, when two-day rainfall was examined, the
264 correlation between accumulated rainfall and drainage area shifts from negative to
265 positive at 10,000 km²; the negative correlation in Figure 3a is only valid for watersheds
266 larger than 10,000 km² (Figure 4a). This transition area increases from 10,000 km² for
267 two-day rainfall to 100,000 km² for four-day rainfall (Figure 4c). The number of

268 watersheds with negative correlation also decreases. Eventually, the weekly rainfall has
269 similar positive correlation with drainage area like antecedent soil moisture (Figure 4f).
270 The increase of transition area may be explained by the increasing response time and
271 confluence time in large watersheds: it takes days to generate flow events by heavy
272 rainfall and for them to reach outlets where it can be observed in large watersheds. This
273 is also consistent with the conclusion in the Yellow River Basin (Ran et al., 2020) and
274 our previous findings of the dominant flood generation mechanism in the middle and
275 lower YZRB: weekly rainfall is the dominant flood driver for sites on the main streams
276 and the major tributaries (Wang et al 2021). The regulated watersheds don't show
277 significant correlation which is understandable for the strong human intervention. For
278 the negative correlation between accumulated rainfall and drainage area at main stream
279 sites, it is difficult to decide whether it is due to scaling effect or human intervention.

280 **3.4 The interlink of watershed characteristics, flood, antecedent soil moisture and** 281 **rainfall**

282 Figure 5 presents the percentile of antecedent soil moisture and rainfall during the
283 AMFs at the study watersheds, the circles are scaled by watershed size and colored with
284 topographic gradient. Except the watersheds with strong human intervention (regulated
285 ones and the ones on main stream), there is a negative correlation between the
286 contribution of rainfall and antecedent soil moisture. The lower right of the scatter are
287 mostly big blue dots, which are large watersheds with gentle topographic gradient. That
288 is, AMFs usually occur when soil moisture is close to saturation while extreme rainfall
289 is not necessary for AMFs in these watersheds. On top of the scatter are relatively small
290 yellow and green dots, those are medium to small watersheds with steep topographic
291 gradient. That is, AMFs are usually generated with extreme rainfall, while the saturation

292 of soil moisture is not necessary. This negative correlation indicates the shift of
293 dominance in AMFs generation from extreme rainfall to antecedent soil wetness from
294 small steep watersheds to large flat ones.

295 Figure 6 shows the relative importance of antecedent soil moisture and rainfall. For
296 the natural watersheds (the circles), SPR increases with drainage area and declines with
297 topographic gradient. That is, the larger the drainage area is, the more essential the
298 contribution of antecedent soil moisture to floods is, and the less influential rainfall is
299 in flood generation. For watersheds with similar drainage area (i.e., the green or light
300 blue dots in Figure 6b), topographic gradient also cast impacts on SPR: SPR decreases
301 with slope. That is, the relative importance of rainfall increases at steeper watersheds.
302 This may be attributed to the shortened hydrological response time due to the steep
303 topography which facilitates rainfall induced floods generation. As a combination of
304 both drainage area and topographic gradient, TWI is positively correlated with SPR at
305 natural watersheds, with less scatter than the correlation between SPR and drainage area
306 or topographic gradient alone. That is, watersheds with larger area and gentler
307 topographic gradient that are easier to get wet tend to have larger SPR: soil wetness is
308 more important in flood generation. There is no significant correlation between SPR
309 and TWI for the regulated watersheds along tributaries (black triangles). However, the
310 sites on main stream show opposite pattern: the SPR at these sites decreases with TWI
311 and drainage area. It is difficult to determine whether this is because of reservoir
312 regulation or not. More data about watersheds larger than 10,000km² but with limited
313 human intervention are needed to examine this hypothesis.

314 Besides TWI, SPR is also correlated with the magnitude of AMF (Figure 7). As
315 Figure 7 shows, the area normalized flood peak declines with flood-generation SPR.

316 Watersheds with large flood peak are mostly the ones with steep topographic gradient
317 and small SPR (i.e., $SPR < 1$) and vice versa. Catchments with more extreme floods are
318 the ones with relatively less influence of soil moisture on flood generation. Similar
319 correlation was also found at event scale in our experimental mountainous watershed,
320 which locates at a headwater of Yangtze River (Liu et al 2021).

321 **4 Discussion**

322 **4.1 The relative importance of antecedent soil moisture and rainfall in flood** 323 **generation**

324 While soil moisture and rainfall are the two main drivers of floods in the middle and
325 lower Yangtze River basin, the dominance of each factor varies across the relatively
326 natural watersheds. Floods in large watersheds are usually generated when soil is almost
327 saturated despite of the relatively small rainfall amount, while extreme rainfall is
328 usually observed during floods in small to medium watersheds (blue dots in Figure 3).
329 The rising contribution of antecedent soil moisture in large watersheds was consistent
330 with the findings in Australian watersheds (Wasko & Nathan, 2019); and the declining
331 influence of rainfall at larger watersheds was also found in Indian watersheds (Garg et
332 al 2019). This contrast correlation with watershed size indicates a shift of dominance in
333 AMFs generation, which may be attributed to the longer confluence time in the large
334 watersheds and less heterogeneity in small watersheds.

335 This shift of dominance can be observed more straightforwardly from the negative
336 correlation between the percentile of rainfall and antecedent soil moisture in Figure 5.
337 The natural watersheds in Figure 5 could be grouped into three classes based on their
338 drainage area and topographic gradient. When a watershed is large and flat, flood

339 occurrence is mainly determined by soil wetness (i.e., the big blue dots at the lower
340 right of the scatter); on the other hand, when a watershed is small and steep, heavy
341 rainfall takes over the dominance (i.e., the small yellow and green dots at the upper left
342 of the scatter). Between these two groups are relatively small watersheds with gentle
343 topographic gradient, where the occurrence of AMF requires both highly saturated soil
344 and relatively heavy rainfall. That is, the dominant influential factor(s) in AMFs
345 generation across watersheds is correlated with the topographic characteristics (i.e.,
346 watershed size and topographic gradient). This helps quantify the relative importance
347 of soil moisture and rainfall in flood generation in the existing work.

348 This shift of dominance is not observed in the main stream sites (i.e., cyan dots in
349 Figure 3), where the percentile of both antecedent soil moisture and precipitation
350 declines with drainage area. This may be attributed to the more complicated flood
351 generation mechanism at large scale as well as the strong human intervention on main
352 stream (e.g., reservoirs, water gates regulation, etc.) (Gao et al., 2018; Long et al., 2020;
353 Zhang et al., 2017). The major responsibilities of reservoirs on the main stream are to
354 reduce peak flow and postpone the time to flood peak (Volpi et al., 2018). As a result,
355 the original flood peak would be delayed by regulation and the actual flood peak would
356 occur when rainfall declines/stops and soil water drains. Another possibility is that
357 when watershed size is larger than 100,000km², the impact of antecedent soil moisture
358 declines as well. To examine this hypothesis, more data from watersheds larger than
359 100,000km² and with limited human intervention is needed. However, this is above the
360 scope of this work and requires future studies.

361 **4.2 Linkage between topographic characteristics, SPR and floods**

362 The correlation between TWI and SPR (Figure 6c) demonstrates that the relative

363 importance of soil moisture and rainfall could be inferred from topographic
364 characteristics quantitatively. We could derive the relative dominance of soil moisture
365 and rainfall in flood generation in specific watershed from its TWI for the natural
366 watersheds without significant human intervention. Rainfall and soil moisture level
367 have been identified as dominant drivers of floods, individually or together, in
368 watersheds worldwide (Berghuijs et al 2016, 2019b; Garg & Mishra 2019; Trambly et
369 al 2021; Ye et al 2017). Our findings provide a framework to quantify the relative
370 importance of rainfall and soil moisture and to further identify the influential factors of
371 their importance based on topographic characteristics that are easy to measure.

372 Meanwhile, the SPR also present a negative correlation with the magnitude of
373 AMFs (Figure 7). That is, we could infer the mean annual AMF based on SPR for each
374 watershed. Since the characteristic SPR could be estimated from TWI, we could derive
375 quantitative estimation of the mean AMFs from topographic characteristics that are easy
376 to measure, even in watersheds with little hydrologic records. There is also similar
377 negative correlation between TWI and AMFs (Figure S2). This would be helpful for
378 flood control management in ungauged watersheds, especially in the mountainous
379 watersheds with risks of flash floods. Similar correlation was also found in the
380 observations from our experimental watershed, a headwater of Yangtze River (Liu et al
381 2021). The ratio of observed antecedent soil moisture and event precipitation also
382 presents similar decline trend with discharge at event scale. However, the correlation
383 between SPR and discharge at event scale is preliminary, more data with higher
384 resolution and detailed analysis are needed for validation at event scale. For this study,
385 our goal is to present the framework to derive flood generation SPR that could be
386 estimated from topographic characteristics and to provide information of mean AMFs.

387 In conclusion, based on the topographic characteristics, we could derive the relative
388 importance of soil moisture and rainfall in flood generation (SPR); and from this
389 relative importance ratio, we could further infer the average flood magnitude at these
390 watersheds. As a result, we could link the topographic characteristics and annual floods
391 through the characteristic SPR during the AMFs.

392 **4.3 Implications**

393 Our findings could be helpful for potential flood risk evaluation in ungauged basins,
394 e.g., headwaters in the mountainous region. With the construction of large reservoirs,
395 the capability of flood risk control has improved substantially along the main stream
396 (Zou et al., 2011; Zhang et al., 2015). However, it is still difficult for quantitative
397 evaluation of flood risk in upstream mountainous watersheds, which are vulnerable to
398 floods but difficult for hydrological modeling and prediction due to little hydrologic
399 records.

400 Our findings suggest that we could derive the flood-generation SPR of each
401 watershed from drainage area and topographic gradient that are easy to measure. The
402 correlation between SPR and flood peak provides information of the mean annual
403 floods in ungauged watersheds. Therefore, in regions without observation data, to build
404 flood control infrastructure such as dams and gates, the mean annual flood peak
405 obtained by SPR based on the topographic characteristics can be used to provide
406 quantitative information for flood control and disaster management. Flood control
407 infrastructures could be designed based on the estimated mean annual flood peak as
408 well as the demographic information. With further validation of this framework at event
409 scale, by using the observed soil moisture from remote sensing data and precipitation
410 forecast to generate real-time prediction of SPR values, we could further provide early

411 warning of floods in these ungauged watersheds. This would be helpful given the
412 increasing possibility of extreme rainfall events due to climate change, however, more
413 data and examination are needed in future studies.

414 **4.4 Limitations**

415 Previous works usually identify the dominant flood generation mechanism based on the
416 comparison of the timing of events (Berghuijs et al 2016; 2019b; Bloschl et al 2017; Ye
417 et al 2017). Similar work has been implemented in our study watersheds, suggesting
418 the importance of soil moisture and rainfall (Wang et al 2021). Based on that, we further
419 looked into the records to quantitatively evaluate the relative importance of soil
420 moisture and rainfall in flood generation. However, there are limitations in our methods.

421 The precipitation data we used were averaged for the study watersheds from 247
422 meteorological stations. Given the large area and considerable spatial heterogeneity, the
423 precipitation data we used may not always be representative of the actual precipitation
424 events. The daily data could also average the rainfall intensity at hourly scale, which
425 could be influential in small mountainous watersheds. ET was scaled as $0.75 \cdot ET_0$ to
426 make sure it is smaller than the potential evaporation. This is a simplified estimation of
427 ET; more sophisticated method is needed in further analysis on specific catchments at
428 event scale.

429 The estimation of soil moisture is also highly simplified, which cannot be
430 considered as precise estimation at event scale. To reduce the influence from this
431 simplification, we used the percentile of soil moisture to represent the relative wetness
432 of soil moisture as well as the seasonal trend of soil moisture, which was then compared
433 with the percentile of rainfall (see supplementary and Figure S3, S4). While more

434 sophisticated models can be used for soil moisture estimation, there could still be
435 substantial uncertainties (Ran et al 2020). Yet the seasonal trend and the relative
436 magnitude, after averaging through long-term records would be less impacted by the
437 simplification in estimation (Berghuijs et al 2019; Zhang et al 2019).

438 Our findings may appear different from that in Yang et al (2020), which attributed
439 the dominant flood generation mechanism in the Yangtze River basin to rainfall. This
440 may be explained by different classification criteria: Yang et al (2020) considered both
441 short-rain and long-rain as rainfall impacts while here we only considered the daily
442 rainfall. Thus, the importance of antecedent soil moisture may be considered as long-
443 rain impacts in Yang et al (2020). It is possible that soil moisture at the day before the
444 AMFs may not be the soil moisture before the event in large catchments due to the long
445 concentration time. We estimated the concentration time for 10 sites with largest
446 drainage area (larger than 100,000 km²): the ones on the main stream and at the outlets
447 of major tributaries following the USBR method (USBR 1973; Gericke & Smithers
448 2014). The concentration time is mostly within two days for main stream sites and is
449 less than 24hr for sites at the outlets of major tributaries (Table S1). Since the rest of
450 the sites are all smaller than these ones, so would be the concentration time. That is, for
451 the natural watersheds we focused on, the concentration time is likely to be within one
452 day. Thus, the soil moisture at the day before AMFs would contribute to the generation
453 of AMFs, and should be applicable for this study.

454 Besides, the exchange with groundwater was not considered in the soil moisture
455 estimation. The exchange with groundwater is more complicated and heterogenous (i.e.,
456 rivers could receive groundwater recharge in hilly area and recharge groundwater in
457 lower land (Che et al 2021)). According to Huang et al. (2021), the variation of

458 groundwater level in the Yangtze River basin is relatively small. Since the goal of this
459 study is to capture the first order seasonal variation of soil moisture and develop a
460 framework that differentiates the relative importance of precipitation and soil moisture
461 in flood generation, in this study, we estimated the soil moisture following Berhuijs (et
462 al 2016, 2019) with a simple water balance equation.

463 Moreover, this work is focused on the relative importance soil moisture and rainfall,
464 the impact of snowmelt is not considered due to the warm and humid climate in the
465 study watersheds. To apply our findings to cold watersheds with significant impact of
466 snow, the snowmelt component needs to be incorporated. In addition, our method is
467 based on the average values from many years. While previous work indicated that the
468 occurrence of floods in our study watersheds are highly concentrated (Wang et al 2021),
469 there could be strong inter-annual variability in other watersheds. In future studies,
470 annual scale and event scale analysis are needed to examine and improve our findings
471 before it can be applied to watersheds with more diverse climate and landscape
472 conditions. There could be uncertainties embedded in the estimation of soil moisture
473 due to the uncertainties in the inputs and model structures. Comprehensive evaluation
474 of the performance and uncertainty is beyond the scope of our study. More sophisticated
475 models with groundwater component, remote sensing data, and reanalysis product with
476 higher spatial-temporal resolution are needed to provide more accurate estimation and
477 further validation of soil moisture, ET, and advances our understandings of the flood-
478 generation SPR.

479 **5 Conclusions**

480 Heavy rainfall on highly saturated soil was identified as the dominant flood generation
481 mechanism across world (Berghuijs et al 2019; Wang et al 2021; Wasko et al 2020).

482 This study aims to further evaluate the relative importance of antecedent soil moisture
483 and rainfall on floods generation and the controlling factors. Climate and hydrological
484 data from 224 hydrological stations and 247 meteorological stations in the middle and
485 lower reaches of the Yangtze River basin was analyzed, along with the modeled soil
486 moisture. Except the regulated watersheds, the relative importance of antecedent soil
487 moisture and daily rainfall present significant correlation with drainage area: the larger
488 the watershed is, the more essential antecedent soil saturation rate is in flood generation,
489 the less important daily rainfall is.

490 Using the percentile of antecedent soil moisture and rainfall as coordinates, the
491 flood generation mechanism(s) of study watersheds could be grouped into three classes:
492 antecedent soil moisture dominated large flat watersheds, heavy rainfall dominated
493 steep and small to middle size watersheds, and small to middle size watersheds with
494 gentle topographic gradient where floods occurrence requires both highly saturated soil
495 and heavy rainfall. Our analysis further shows that the ratio of relative importance
496 between antecedent soil moisture and rainfall (SPR) can be predicted by topographic
497 wetness index. When the topographic wetness index is large, the dominance of
498 antecedent soil moisture for extreme floods is stronger, and *vice versa*. The SPR also
499 presents negative correlation with area normalized flood peak.

500 With the potential increase of extreme rainfall events (Gao et al., 2016; Chen et al.,
501 2016), upstream mountainous watersheds in the middle and lower Yangtze River basin
502 are facing higher risk of extreme floods. The lack of hydrological records further
503 increases the vulnerability of people in these watersheds. The flood risks could be
504 reduced by construction of flood control facilities, but it is difficult to set flood control
505 standards in these ungauged watersheds. Our findings provide a framework to

506 quantitatively estimate the possible flood risk for these ungauged watersheds. Based on
507 measurable watershed characteristics (i.e., drainage area and topographic gradient), the
508 flood generation SPR could be derived, which could then be used to estimate the mean
509 annual flood. This information can provide scientific support for flood control
510 management as well as infrastructures construction.

511 Future analysis at event scale could help generate the flood-generation curve
512 between SPR and discharge at event scale to further improve flood risk predictions in
513 these small ungauged watersheds. With more data from other regions and improved
514 estimation or observation of soil moisture, we could expand our analysis to watersheds
515 with more diverse climate and topographic characteristics to examine and refine our
516 findings and to enhance our understandings of flood generation. Comparison between
517 different time periods (i.e., before and after 2000) could also reveal temporal changes
518 in flood generation, which may be linked to climate change, yet longer data records are
519 needed to generate representative patterns.

520 **Data availability**

521 DEM data was downloaded from Geospatial Data Cloud at <http://www.gscloud.cn/>.
522 Climatological data used in this study was obtained from China Meteorological Data
523 Network, which can be accessed at <http://data.cma.cn/>. Discharge data comes from
524 Annual Hydrological Report of the People's Republic of China issued by Yangtze River
525 Water Resources Commission.

526

527 **Author contributions**

528 QR and SY conceptualized the original idea and designed the work, JW conducted the
529 data analysis, XC and LL contributed to data collection and preparation, JL conducted
530 additional analysis during the revision, QR, JW, and SY wrote the manuscript.

531 **Competing interests**

532 The contact author has declared that none of the authors has any competing interests.

533

534 **Acknowledgements**

535 This research was funded by the National Key Research and Development Program of
536 China (2019YFC1510701-01), and National Natural Science Foundation of China
537 (51979243).

538

539 **References**

540 Abbas, S.A., Xuan, Y. and Song, X.: Quantile Regression Based Methods for
541 Investigating Rainfall Trends Associated with Flooding and Drought Conditions.
542 Water Resources Management, 33(12), 4249-4264, [https://doi:10.1007/s11269-](https://doi:10.1007/s11269-019-02362-0)
543 019-02362-0, 2019.

544 Alfonso R., Nilza M. R.C., and Anderson L. R.: Numerical Modelling of the
545 Topographic Wetness Index: An Analysis at Different Scales, International
546 Journal of Geosciences(4), 476-483, <https://doi:10.4236/ijg.2011.24050>, 2011.

547 Allen R. G., Pereira L. S. and Raes D.: Crop evapotranspiration-Guidelines for
548 computing crop water requirements FAO Irrigation and drainage paper
549 NO.56(Electric Publication)[M], Rome , Italy:FAO, 1998.

550 Bennett, B., Leonard, M., Deng, Y., Westra, S.: An empirical investigation into the
551 effect of antecedent precipitation on flood volume. J. Hydrol. 567, 435–445.
552 <https://doi.org/10.1016/j.jhydrol.2018.10.025>, 2018.

553 Berghuijs, W.R., Allen, S.T., Harrigan, S. and Kirchner, J.W.: Growing Spatial Scales
554 of Synchronous River Flooding in Europe. Geophysical Research Letters, 46(3),
555 1423-1428, <https://doi:10.1029/2018GL081883>, 2019a.

556 Berghuijs, W.R., Harrigan, S., Molnar, P., Slater, L.J. and Kirchner, J.W.: The Relative
557 Importance of Different Flood-Generating Mechanisms Across Europe. Water
558 Resources Research, 55(6), 4582-4593, <https://doi:10.1029/2019WR024841>,
559 2019b.

560 Berghuijs, W.R., Woods, R.A., Hutton, C.J. and Sivapalan, M.: Dominant flood
561 generating mechanisms across the United States. Geophysical Research Letters,
562 43(9), 4382-4390, <https://doi:10.1002/2016GL068070>, 2016.

563 Bertola, M., Viglione, A., Vorogushyn, S., Lun, D., Merz, B., Blöschl, G.: Do small
564 and large floods have the same drivers of change? A regional attribution analysis

565 in Europe. *Hydrol. Earth Syst. Sci.* 25, 1347–1364. <https://doi.org/10.5194/hess->
566 25-1347-2021, 2021.

567 Blöschl, G., Nester, T., Komma, J., Parajka, J. and Perdigao, R.A.P.: The June 2013
568 flood in the Upper Danube Basin, and comparisons with the 2002, 1954, and 1899
569 floods. *Hydrol. Earth Syst. Sci.*, 17, 5197–5212, 2013.

570 Blöschl, G., Hall, J., Parajka, J., Perdigão, R. A., Merz, B., Arheimer, B., et al.:
571 Changing climate shifts timing of European floods. *Science*, 357(6351), 588 –
572 590. <https://doi.org/10.1126/science.aan2506>, 2017.

573 Blöschl, G., Hall, J., Viglione, A., Perdigao, R.A., Parajka, J., Merz, B., et al.: Changing
574 climate both increases and decreases European river floods, *Nature*, 573, 108 –
575 111, 2019.

576 Berti, A., Tardivo, G., Chiaudani, A., Rech, F. and Borin, M.: Assessing reference
577 evapotranspiration by the Hargreaves method in north-eastern Italy. *Agricultural*
578 *Water Management*, 140, 20-25, <https://doi:10.1016/j.agwat.2014.03.015>, 2014.

579 Brunner, M. I., Seibert, J. and Favre, A.C.: Bivariate return periods and their importance
580 for flood peak and volume estimation. *Wire's Water*, 3, 819 – 833.
581 <https://doi.org/10.1002/wat2.1173>, 2016.

582 Brunner, M. I., Gilleland, E., Wood, A., Swain, D. L., and Clark, M.: Spatial
583 dependence of floods shaped by spatiotemporal variations in meteorological and
584 land - surface processes. *Geophysical Research Letters*, 47, e2020GL088000.
585 <https://doi.org/10.1029/2020GL088000>, 2020.

586 Brunner, M. I., Swain, D. L., Wood, R.R. et al. An extremeness threshold determines
587 the regional response of floods to changes in rainfall extremes. *Commun Earth*
588 *Environ* 2, 173. <https://doi.org/10.1038/s43247-021-00248-x>, 2021.

589 Cai, Q. H.: Great protection of Yangtze River and watershed ecology, *Yangtze River*
590 (01), 70-74, <https://doi:10.16232/j.cnki.1001-4179.2020.01.011>, 2020.

591 Cen, S.-x., Gong, Y.-f., Lai, X. and Peng, L.: The Relationship between the
592 Atmospheric Heating Source/Sink Anomalies of Asian Monsoon and
593 Flood/Drought in the Yangtze River Basin in the Meiyu Period. *Journal of*
594 *Tropical Meteorology*, 21(4), 352-360, 2015.

595 Che, Q., Su, X., Zheng, S., Li, Y.: Interaction between surface water and groundwater
596 in the Alluvial Plain (anqing section) of the lower Yangtze River Basin:
597 environmental isotope evidence. *Journal of Radioanalytical and Nuclear*
598 *Chemistry*, 329, 1331–1343, 2021.

599 Chen, Y. and Zhai, P.: Mechanisms for concurrent low-latitude circulation anomalies
600 responsible for persistent extreme precipitation in the Yangtze River Valley.
601 *Climate Dynamics*, 47(3-4), 989-1006, <https://doi:10.1007/s00382-015-2885-6>,
602 2016.

603 CRED (2015). The human cost of natural disasters: A global perspective: Centre for
604 research on the epidemiology of disasters.

605 Deb, P., Kiem, A.S. and Willgoose, G.: Mechanisms influencing non-stationarity in
606 rainfall-runoff relationships in southeast Australia. *Journal of Hydrology*, 571,
607 749-764, <https://doi:10.1016/j.jhydrol.2019.02.025>, 2019.

608 Desai, B., Maskrey, A., Peduzzi, P., De Bono, A., & Herold, C. Making Development
609 Sustainable: The Future of Disaster Risk Management. Global Assessment Report
610 on Disaster Risk Reduction <http://archive-ouverte.unige.ch/unige:78299> (UNISDR,
611 2015).

612 Do, H. X., Mei, Y., & Gronewold, A. D.: To what extent are changes in flood magnitude
613 related to changes in precipitation extremes? *Geophysical Research Letters*, 47,
614 e2020GL088684. <https://doi.org/10.1029/2020GL088684>, 2020.

615 Fang, X. and Pomeroy, J.W.: Impact of antecedent conditions on simulations of a flood
616 in a mountain headwater basin. *Hydrological Processes*, 30(16), 2754-2772,
617 <https://doi:10.1002/hyp.10910>, 2016.

618 Feng, B. F., Dai M. L. and Zhang T.: Effect of Reservoir Group Joint Operation on
619 Flood Control in the Middle and Lower Reaches of Yangtze River, *Journal of*
620 *Water Resources Research* (3), 278-284, <https://doi:10.12677/JWRR.2017.63033>,
621 2017.

622 Fu, G., Yu, J., Yu, X., Ouyang, R., Zhang, Y., Wang, P., Liu, W. and Min, L.: Temporal
623 variation of extreme rainfall events in China, 1961-2009. *Journal of Hydrology*,
624 487, 48-59, <https://doi:10.1016/j.jhydrol.2013.02.021>, 2013.

625 Gao, T. and Xie, L.: Spatiotemporal changes in precipitation extremes over Yangtze
626 River basin, China, considering the rainfall shift in the late 1970s. *Global and*

627 Planetary Change, 147, 106-124, <https://doi:10.1016/j.gloplacha.2016.10.016>,
628 2016.

629 Gao, Y., Wang, H., Lu, X., Xu, Y., Zhang, Z. and Schmidt, A.R.: Hydrologic Impact
630 of Urbanization on Catchment and River System Downstream from Taihu Lake.
631 Journal of Coastal Research, 82-88, <https://doi:10.2112/SI84-012.1>, 2018.

632 Garg, S., & Mishra, V.: Role of extreme precipitation and initial hydrologic conditions
633 on floods in Godavari river basin, India. Water Resources Research, 55, 9191 -
634 9210. <https://doi.org/10.1029/2019WR025863>, 2019.

635 Grabs, T., Seibert, J., Bishop, K. and Laudon, H.: Modeling spatial patterns of saturated
636 areas: A comparison of the topographic wetness index and a dynamic distributed
637 model. Journal of Hydrology, 373(1-2), 15-23,
638 <https://doi:10.1016/j.jhydrol.2009.03.031>, 2009.

639 Huang, C., Zhou, Y., Zhang, S., Wang, J., Liu, F., Gong, C., Yi, C., Li, L., Zhou, H.,
640 Wei, L., Pan, X., Shao, C., Li, Y., Han, W., Yin, Z., and Li, X.: Groundwater
641 resources in the Yangtze River Basin and its current development and utilization[J].
642 Geology of China, 2021, 48(4):979-1000.

643 IPCC. Managing the Risks of Extreme Events and Disasters to Advance Climate
644 Change Adaptation (eds Field, C. B. et al.) (Cambridge Univ. Press, 2012).

645 Kato, K.: On the Abrupt Change in the Structure of the Baiu Front over the China
646 Continent in Late May of 1979. Journal of the Meteorological Society of Japan,
647 63(1), 20-36, https://doi:10.2151/jmsj1965.63.1_20, 1985.

648 Kazuki, T., Oliver C. S. V., Masahiro, R.: Spatial variability of precipitation and soil
649 moisture on the 2011 flood at chao phraya river basin. International Water
650 Technology Association, Proceedings of Hydrology and Water Resources, B, 17-
651 21, 2013.

652 Kemter, M., Merz, B., Marwan, N., Vorogushyn, S., & Blöschl, G.: Joint trends in flood
653 magnitudes and spatial extents across Europe. Geophysical Research Letters, 47,
654 e2020GL087464. <https://doi.org/10.1029/2020GL087464>, 2020.

655 Lehner, B., C. Reidy Liermann, C. Revenga, C. Vörösmarty, B. Fekete, P. Crouzet, P.
656 Döll, M. Endejan, K. Frenken, J. Magome, C. Nilsson, J.C. Robertson, R. Rodel,
657 N. Sindorf, and D. Wisser. 2011. High-resolution mapping of the world's
658 reservoirs and dams for sustainable river-flow management. Frontiers in Ecology
659 and the Environment 9 (9): 494-502.

-
- 660 Li, Q., Wei, F. and Li, D.: Interdecadal variation of East Asian summer monsoon and
661 drought/flood distribution over eastern China in the last 159 years. *Journal of*
662 *Geographical Sciences*, 21(4), 579-593, <https://doi:10.1007/s11442-011-0865-2>,
663 2011.
- 664 Li, X., Zhang, K., Gu, P., Feng, H., Yin, Y., Chen, W. and Cheng, B.: Changes in
665 precipitation extremes in the Yangtze River Basin during 1960-2019 and the
666 association with global warming, ENSO, and local effects. *Science of the Total*
667 *Environment*, 760, <https://doi:10.1016/j.scitotenv.2020.144244>, 2021.
- 668 Liu, B., Yan, Y., Zhu, C., Ma, S., & Li, J.: Record - breaking Meiyu rainfall around the
669 Yangtze River in 2020 regulated by the subseasonal phase transition of the North
670 Atlantic Oscillation. *Geophysical Research Letters*, 47, e2020GL090342.
671 <https://doi.Org/10.1029/2020GL090342>, 2020.
- 672 Liu, L., Ye, S., Chen, C., Pan, H. and Ran, Q.: Nonsequential Response in Mountainous
673 Areas of Southwest China. *Frontiers in Earth Science*, 9: 1-15. doi:
674 10.3389/feart.2021.660244, 2021
- 675 Liu, N., Jin, Y. and Dai, J.: Variation of Temperature and Precipitation in Urban
676 Agglomeration and Prevention Suggestion of Waterlogging in Middle and Lower
677 Reaches of Yangtze River. 3rd International Conference on Energy Equipment
678 Science and Engineering (Iceese 2017), 128, [https://doi:10.1088/1755-](https://doi:10.1088/1755-1315/128/1/012165)
679 1315/128/1/012165, 2018.
- 680 Liu, S., Huang, S., Xie, Y., Wang, H., Leng, G., Huang, Q., Wei, X., and Wang, L.:
681 Identification of the Non-stationarity of Floods: Changing Patterns, Causes, and
682 Implications, *Water Resour. Manag.*, 33, 939–953, 2018.
- 683 Liu, Y., Xinyu, L., Liancheng, Z., Yang, L., Chunrong, J., Ni, W. and Juan, Z.:
684 Quantifying rain, snow and glacier meltwater in river discharge during flood
685 events in the Manas River Basin, China. *Natural Hazards*, 108(1), 1137-1158,
686 <https://doi:10.1007/s11069-021-04723-8>, 2021.
- 687 Long, L.H., Ji, D.B., Yang, Z.Y., Cheng, H.Q., Yang, Z.J., Liu, D.F., Liu, L. and Lorke,
688 A.: Tributary oscillations generated by diurnal discharge regulation in Three
689 Gorges Reservoir. *Environmental Research Letters*, 15(8),
690 <https://doi:10.1088/1748-9326/ab8d80>, 2020.
- 691 Lu, M., Wu, S.-J., Chen, J., Chen, C., Wen, Z. and Huang, Y.: Changes in extreme
692 precipitation in the Yangtze River basin and its association with global mean

693 temperature and ENSO. *International Journal of Climatology*, 38(4), 1989-2005,
694 <https://doi:10.1002/joc.5311>, 2018.

695 Meles, M.B., Younger, S.E., Jackson, C.R., Du, E., Drover, D.: Wetness index based
696 on landscape position and topography (WILT): Modifying TWI to reflect
697 landscape position, *Journal of Environmental Management* 255, 109863, 2020.

698 Miao, Q., Huang, M. and Li, R., Q.: Response of net primary productivity of vegetation
699 in Yangtze River Basin to future climate change. *Journal of Natural Resources*, 25,
700 08(2010):1296-1305, doi:CNKI:SUN:ZRZX.0.2010-08-007, 2015.

701 Munoz, S.E., Giosan, L., Therrell, M.D., Remo, J.W.F., Shen, Z., Sullivan, R.M.,
702 Wiman, C., O'Donnell, M., and Donnelly, J.P.: Climatic control of Mississippi
703 River flood hazard amplified by river engineering, 556, 95 – 98, 2018.

704 Musselman, K.N., Lehner, F., Ikeda, K., Clark, M.P., Prein, A.F., Liu, C., Barlage, M.
705 and Rasmussen, R.: Projected increases and shifts in rain-on-snow flood risk over
706 western North America, *Nature Climate Change*, 8, 808 – 812, 2018.

707 Ockert J. G. and Jeff C. S.: Review of methods used to estimate catchment response
708 time for the purpose of peak discharge estimation, *Hydrological Sciences Journal*,
709 59:11, 1935-1971, DOI: 10.1080/02626667.2013.866712, 2014.

710 Ohmura, A. and Wild, M.: Is the hydrological cycle accelerating? *Science*, 298, 1345 –
711 1346, 2002.

712 Pegram, G. and Bardossy, A.: Downscaling Regional Circulation Model rainfall to
713 gauge sites using recorelation and circulation pattern dependent quantile-quantile
714 transforms for quantifying climate change. *Journal of Hydrology*, 504, 142-159,
715 <https://doi:10.1016/j.jhydrol.2013.09.014>, 2013.

716 Peng, T., Tian, H., Singh, V. P., Chen, M., Liu, J., Ma, H. B. and Wang, J. B.:
717 Quantitative assessment of drivers of sediment load reduction in the Yangtze River
718 basin, China, *Journal of Hydrology*, 580,
719 <https://doi:10.1016/j.jhydrol.2019.124242>, 2020.

720 Qian, H. and Xu, S.-B.: Prediction of Autumn Precipitation over the Middle and Lower
721 Reaches of the Yangtze River Basin Based on Climate Indices. *Climate*, 8(4),
722 <https://doi:10.3390/cli8040053>, 2020.

723 Ran, Q., Chen, X., Hong Y., Ye S., and Gao J.: Impacts of terracing on hydrological
724 processes: A case study from the Loess Plateau of China. *Journal of Hydrology*,
725 588, <https://doi:10.1016/j.jhydrol.2020.125045>, 2020.

-
- 726 Ran, Q., Zong, X., Ye, S., Gao, J. and Hong, Y.: Dominant mechanism for annual
727 maximum flood and sediment events generation in the Yellow River basin. *Catena*,
728 187, <https://doi:10.1016/j.catena.2019.104376>, 2020.
- 729 Ray S. M., Ramakar J. and Kishanjit K. K.: Precipitation-runoff simulation for a
730 Himalayan River Basin, India using artificial neural network algorithms, *Sciences*
731 *in Cold and Arid Regions*, 5(1), 85-95, 2013.
- 732 Rottler, E., Francke, T., Burger, G., and Bronstert, A.: Long-term changes in central
733 European river discharge for 1869 – 2016: impact of changing snow covers,
734 reservoir constructions and an intensified hydrological cycle, *Hydrol. Earth Syst.*
735 *Sci.*, 24, 1721 – 1740, 2020.
- 736 Smith, J. A., Cox, A. A., Baeck, M. L., Yang, L., and Bates, P.: Strange floods: the
737 upper tail of flood peaks in the United States, *Water Resour. Res.*, 54, 6510 – 6542,
738 2018.
- 739 Sorensen, R., Zinko, U., and Seibert, J.: On the calculation of the topographic wetness
740 index: evaluation of different methods based on field observations, *Hydrology and*
741 *Earth System Sciences*, 10, 101–112, 2006.
- 742 Su, Z., Ho, M., Hao, Z., Lall, U., Sun, X., Chen, X. and Yan, L.: The impact of the
743 Three Gorges Dam on summer streamflow in the Yangtze River Basin.
744 *Hydrological Processes*, 34(3), 705-717, <https://doi:10.1002/hyp.13619>, 2020.
- 745 Suresh, S. S., Benefit O., Augustine T., and Trevor P.: Peoples' Perception on the
746 Effects of Floods in the Riverine Areas of Ogbia Local Government Area of
747 Bayelsa State, Nigeria, *Knowledge Management*, [https://doi:10.18848/2327-](https://doi:10.18848/2327-7998/CGP/v12i02/50793)
748 [7998/CGP/v12i02/50793](https://doi:10.18848/2327-7998/CGP/v12i02/50793), 2013.
- 749 Tao, S. Y., *Rainstorm in China* [M], Beijing: Science Press, 1980.(in Chinese)
- 750 Trambly, Y., Villarini, G., El Khalki, E. M., Gründemann, G., & Hughes, D.:
751 Evaluation of the drivers responsible for flooding in Africa. *Water Resources*
752 *Research*, 57, e2021WR029595. <https://doi.Org/10.1029/2021WR029595>, 2021.
- 753 USBR (United States Bureau of Reclamation), 1973. *Design of small dams*. 2nd ed.
754 Washington, DC: Water Resources Technical Publications.
- 755 Vicente-Serrano, S.M., Azorin-Molina, C., Sanchez-Lorenzo, A., Revuelto, J., Lopez-
756 Moreno, J.I., Gonzalez-Hidalgo, J.C., Moran-Tejeda, E. and Espejo, F.: Reference
757 evapotranspiration variability and trends in Spain, 1961-2011. *Global and*
758 *Planetary Change*, 121, 26-40, <https://doi:10.1016/j.gloplacha.2014.06.005>, 2014.

-
- 759 Volpi, E., Di Lazzaro, M., Bertola, M., Viglione, A. and Fiori, A.: Reservoir Effects on
760 Flood Peak Discharge at the Catchment Scale. *Water Resources Research*, 54(11),
761 9623-9636, <https://doi:10.1029/2018wr023866>, 2018.
- 762 Wang, H., Zhou, Y., Pang, Y. and Wang, X.: Fluctuation of Cadmium Load on a Tide-
763 Influenced Waterfront Lake in the Middle-Lower Reaches of the Yangtze River.
764 *Clean-Soil Air Water*, 42(10), 1402-1408, <https://doi:10.1002/clen.201300693>,
765 2014.
- 766 Wang, J., Ran, Q., Liu, L., Pan, H. and Ye, S.: Study on the Dominant Mechanism of
767 Extreme Flow Events in the Middle and Lower Reaches of the Yangtze River,
768 *China Rural Water and Hydropower*, Accepted.
- 769 Wang, R., Yao, Z., Liu, Z., Wu, S., Jiang, L. and Wang, L.: Snow cover variability and
770 snowmelt in a high-altitude ungauged catchment. *Hydrological Processes*, 29(17),
771 3665-3676, <https://doi:10.1002/hyp.10472>, 2015.
- 772 Wang, W., Xing W., Yang, T., Shao, Q., Peng, S., Yu, Z., and Yong, B.: Characterizing
773 the changing behaviours of precipitation concentration in the Yangtze River Basin,
774 China. *Hydrological Processes*, 27(24), 3375-3393, <https://doi:10.1002/hyp.9430>,
775 2013.
- 776 Wang, Z. and Plate, E.: Recent flood disasters in China. *Proceedings of the Institution*
777 *of Civil Engineers – Water and Maritime Engineering* (3),
778 <https://doi:10.1680/wame.2002.154.3.177>, 2002.
- 779 Wasko, C. and Nathan, R.: Influence of changes in rainfall and soil moisture on trends
780 in flooding. *Journal of Hydrology*, 575, 432-441,
781 <https://doi:10.1016/j.jhydrol.2019.05.054>, 2019.
- 782 Wasko, C., Nathan, R., & Peel, M. C.: Changes in antecedent soil moisture modulate
783 flood seasonality in a changing climate. *Water Resources Research*, 56,
784 e2019WR026300. <https://doi.org/10.1029/2019WR026300>, 2020.
- 785 Wasko, C., Nathan, R., Stein, L., O’Shea, D.: Evidence of shorter more extreme
786 rainfalls and increased flood variability under climate change. *J. Hydrol.* 603,
787 126994. <https://doi.org/10.1016/j.jhydrol.2021.126994>, 2021.
- 788 Wu, X. S., Guo, S. L. and Ba, H. H.: Long-term precipitation forecast method based on
789 SST multipole index, *Journal of water conservancy*(10), 1276-1283,
790 <https://doi:10.13243/j.cnki.slxb.20180544>, 2018.

-
- 791 Xia, J. and Chen, J.: A new era of flood control strategies from the perspective of
792 managing the 2020 Yangtze River flood. *Science China-Earth Sciences*, 64(1), 1-
793 9, <https://doi:10.1007/s11430-020-9699-8>, 2021.
- 794 Xie, Z., Du, Y., Zeng, Y. and Miao, Q.: Classification of yearly extreme precipitation
795 events and associated flood risk in the Yangtze-Huaihe River Valley. *Science*
796 *China-Earth Sciences*, 61(9), 1341-1356, <https://doi:10.1007/s11430-017-9212-8>,
797 2018.
- 798 Yang, H.F., Yang, S.L., Xu, K.H., Milliman, J.D., Wang, H., Yang, Z., Chen, Z. and
799 Zhang, C.Y.: Human impacts on sediment in the Yangtze River: A review and new
800 perspectives. *Global and Planetary Change*, 162, 8-17,
801 <https://doi:10.1016/j.gloplacha.2018.01.001>, 2018.
- 802 Yang, L., Wang, L., Li, X. and Gao, J.: On the flood peak distributions over China.
803 *Hydrology and Earth System Sciences*, 23(12), 5133-5149,
804 <https://doi:10.5194/hess-23-5133-2019>, 2019.
- 805 Yang, W., Yang, H., and Yang, D.: Classifying floods by quantifying driver
806 contributions in the Eastern Monsoon Region of China, *Journal of Hydrology*, 585,
807 124767, 2020.
- 808 Yang, W., Yang, H., Yang, D., and Hou, A.: Causal effects of dams and land cover
809 changes on flood changes in mainland China. *Hydrol. Earth Syst. Sci.*, 25, 2705–
810 2720, 2021.
- 811 Ye, S., Li, H., Leung, L.R., Guo, J., Ran, Q., Demissie, Y., et al., 2017. Understanding
812 flood seasonality and its temporal shifts within the contiguous United States. *J.*
813 *Hydrometeorol.* 18 (7), 1997 – 2009.
- 814 Ye, X., Xu, C.-Y., Li, Y., Li, X. and Zhang, Q.: Change of annual extreme water levels
815 and correlation with river discharges in the middle-lower Yangtze River:
816 Characteristics and possible affecting factors. *Chinese Geographical Science*, 27(2),
817 325-336, <https://doi:10.1007/s11769-017-0866-x>, 2017.
- 818 Yu, F., Chen, Z., Ren, X. and Yang, G.: Analysis of historical floods on the Yangtze
819 River, China: Characteristics and explanations. *Geomorphology*, 113(3-4), 210-
820 216, <https://doi:10.1016/j.geomorph.2009.03.008>, 2009.
- 821 Zhang, H., Liu, S., Ye, J. and Yeh, P.J.F.: Model simulations of potential contribution
822 of the proposed Huangpu Gate to flood control in the Lake Taihu basin of China.

823 Hydrology and Earth System Sciences, 21(10), 5339-5355,
824 <https://doi:10.5194/hess-21-5339-2017>, 2017.

825 Zhao, J., Li, J., Yan, H., Zheng, L. and Dai, Z.: Analysis on the Water Exchange
826 between the Main Stream of the Yangtze River and the Poyang Lake. 2011 3rd
827 International Conference on Environmental Science and Information Application
828 Technology Esiat 2011, Vol 10, Pt C,10, 2256-2264,
829 <https://doi:10.1016/j.proenv.2011.09.353>, 2011.

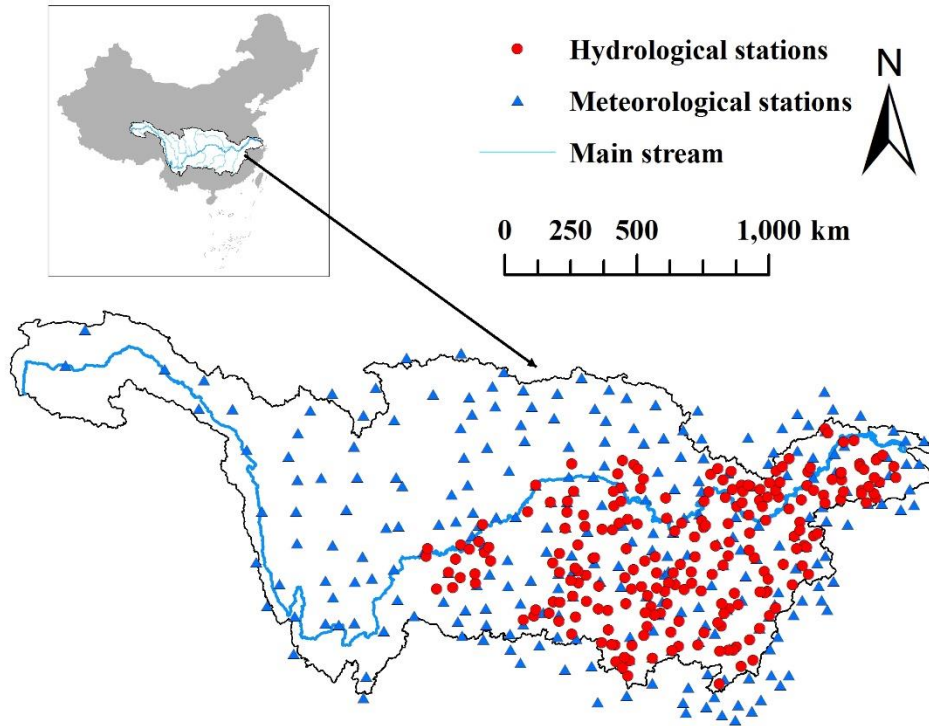
830 Zhang, S., Kang, L. and He, X.: Equal proportion flood retention strategy for the leading
831 multireservoir system in upper Yangtze River. International Conference on Water
832 Resources and Environment, WRE 2015, 2015.

833 Zhang, W., Villarini, G., Vecchi, G.A. and Smith, J. A.: Urbanization exacerbated the
834 rainfall and flooding caused by hurricane Harvey in Houston. *Nature*, 563, 384 –
835 388, 2018.

836 Zhang, K., Wang, Q., Chao, L., Ye, J., Li, Z., Yu, Z., Yang, T. and Ju, Q.: Ground
837 observation-based analysis of soil moisture spatiotemporal variability across a
838 humid to semi-humid transitional zone in China. *Journal of Hydrology*, 574, 903-
839 914, 2019.

840 Zou, B., Li, Y., Feng, B.: Analysis on dispatching influence of Three Gorges Reservoir
841 on water level of main stream in mid-lower reaches of Yangtze River: a case study
842 of flood in July,2010. *Yangtze River*, 42.06:80-82+100. doi:10.16232/j.cnki.1001-
843 4179.2011.06.004, 2011.

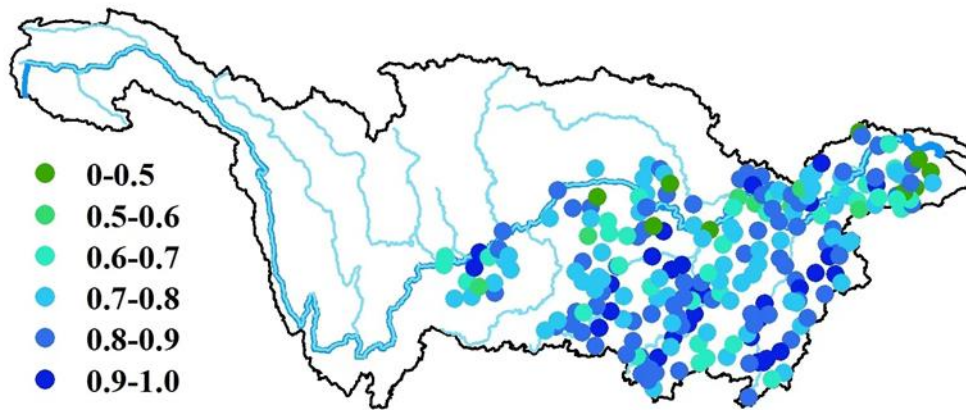
844
845



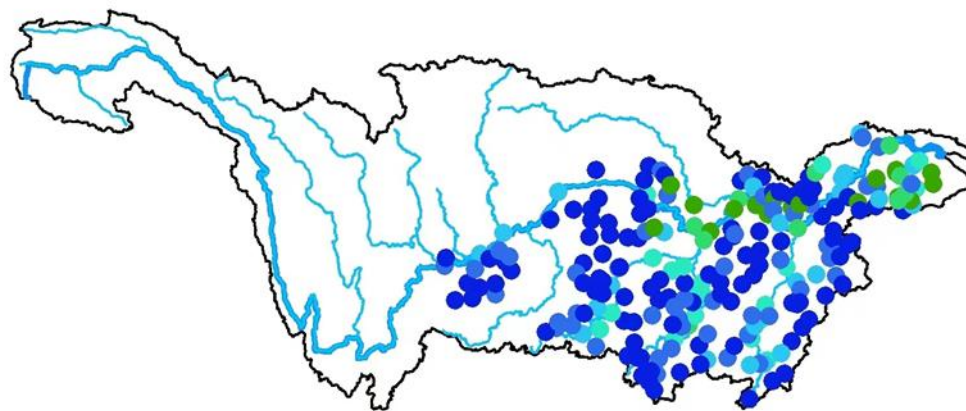
846

847 **Figure 1:** Map of the Yangtze River basin, and the meteorological stations and
848 hydrological stations. The blue line is the main stream of Yangtze River.

849



(a) Percentile of antecedent soil moisture

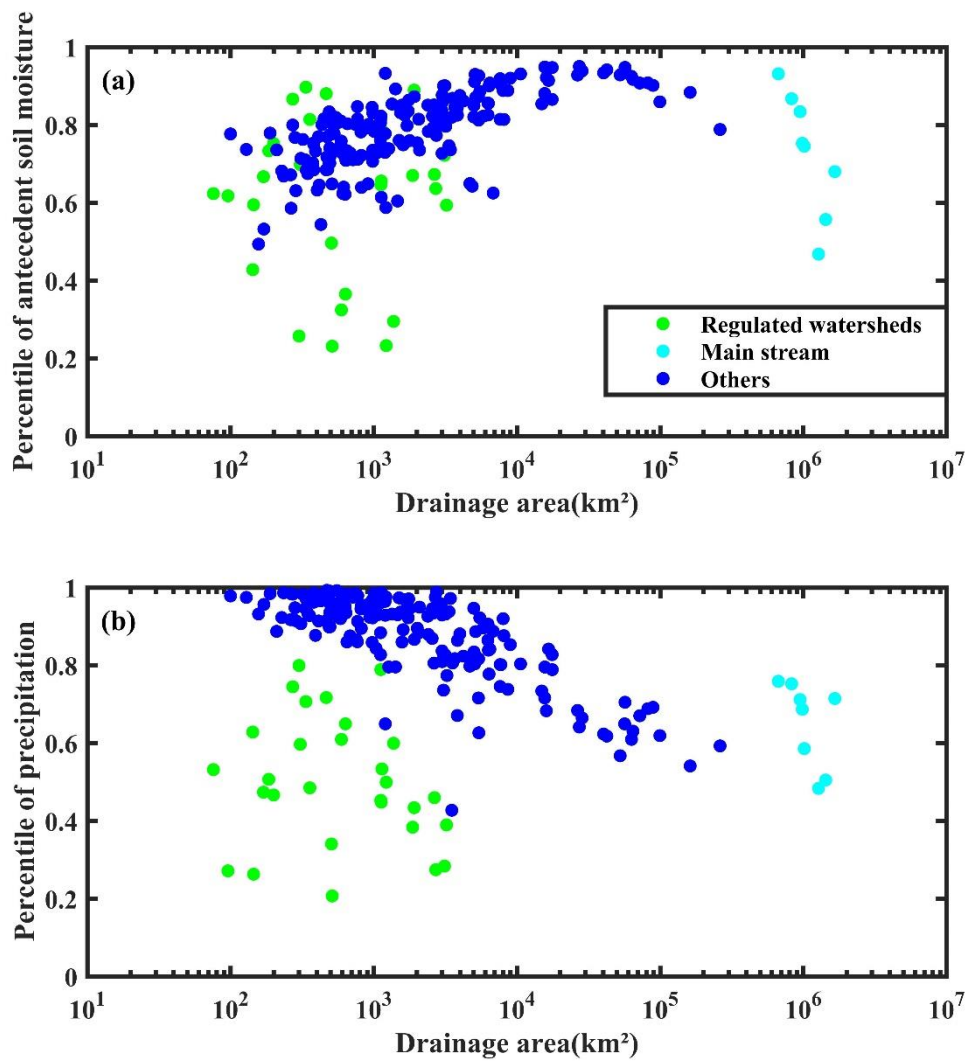


(b) Percentile of precipitation

850

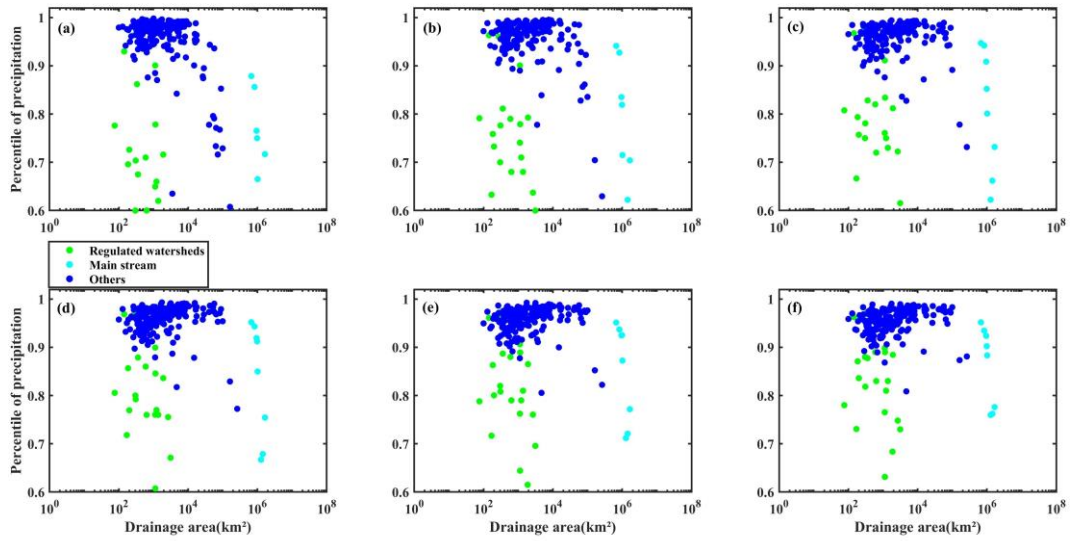
851 **Figure 2:** The spatial distribution of (a) the percentile of antecedent soil moisture during
 852 annual maximum flood; (b) the percentile of daily precipitation during annual
 853 maximum flood.

854



855
 856 **Figure 3:** Scatterplot between the drainage area and (a) the percentile of antecedent soil
 857 moisture of AMF events (the linear regression for blue dots: $R^2 = 0.46$, p -value < 0.001);
 858 (b) the percentile of precipitation at the day of AMF events (the linear regression for
 859 blue dots: $R^2 = 0.61$, p -value < 0.001). The green dots represent the regulated watershed,
 860 the cyan dots represent the sites on the main stream, and the rest sites are shown in blue.

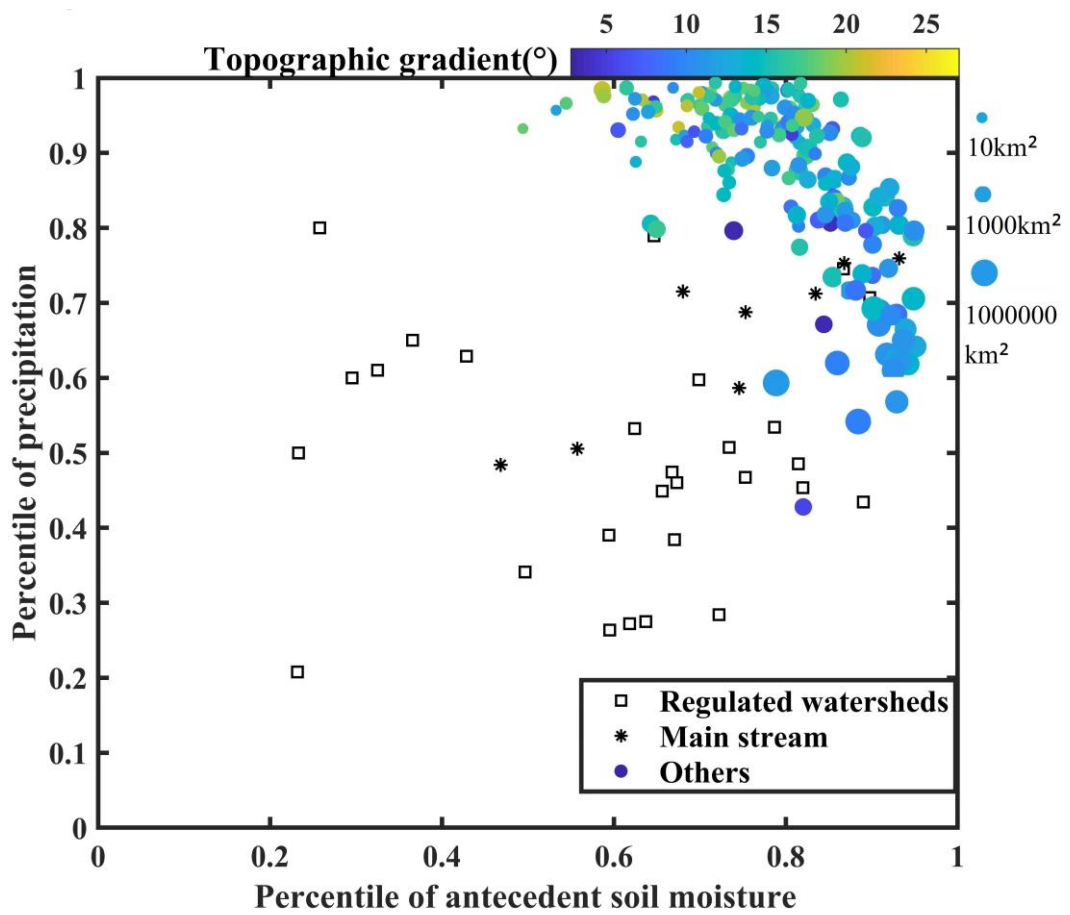
861
 862
 863



864

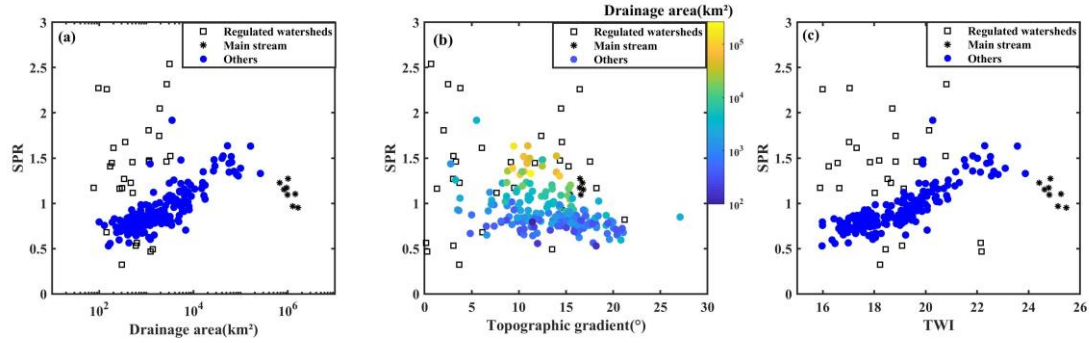
865 **Figure 4:** Scatterplot between the drainage area and the percentile of accumulated
 866 rainfall of (a) two days; (b) three days; (c) four days; (d) five days; (e) six days; and (f)
 867 seven days on AMF events.

868



869
 870
 871
 872
 873

Figure 5: Scatterplot of the percentile of precipitation and antecedent soil moisture, the color represents topographic gradient and the size of circles is scaled by drainage area.



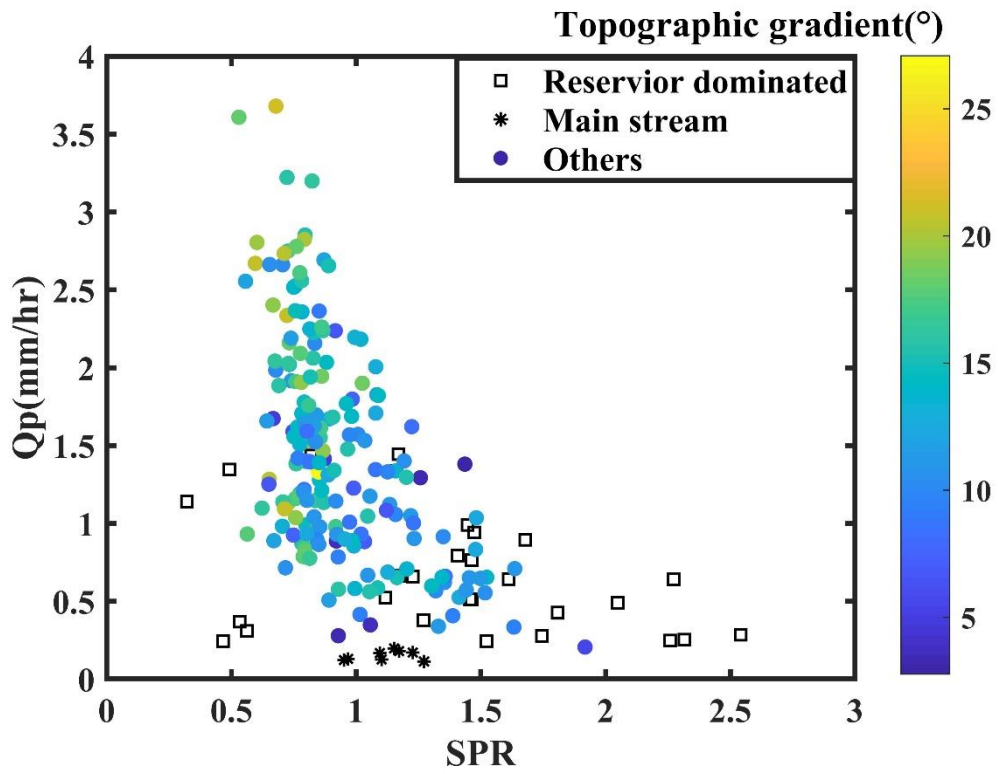
874

875 **Figure 6:** Scatterplots between the ratio of antecedent soil moisture and precipitation

876 (SPR) and (a) drainage area; (b) topographic gradient; and (c) topographic wetness

877 index (TWI).

878



879

880 **Figure 7:** Scatterplot between the ratio of antecedent soil moisture and precipitation
 881 (SPR) and area weighted annual maximum discharge (Q_p), the color represents
 882 topographic gradient.